MAPPING A SPACE MANIPULATOR TO A DYNAMICALLY EQUIVALENT MANIPULATOR

Bin Liang Yangsheng Xu Marcel Bergerman

CMU-RI-TR-96-33

The Robotics Institute
Carnegie Mellon University
Pittsburgh, Pennsylvania 15213

September, 1996

This research is partially sponsored by the Brazilian National Council for Research and Development (CNPq). The views and conclusions contained in this document are those of the authors and should not be interpreted as representing the official policies or endorsements, either expressed or implied, of CNPq or Carnegie Mellon University.

Table of Contents

List of Figures

List of Tables

Abstract

In this paper, we discuss the problem of how a free-floating space manipulator can be mapped to a conventional, fixed-base manipulator which preserves both its dynamic and kinematic properties. This manipulator is called dynamically equivalent manipulator (DEM). The DEM concept not only allows us to model a free-floating space manipulator system with simple, well-understood methods, but also can be physically built using a conventional manipulator system to experimentally study the dynamic performance and task execution of a space manipulator system, without having to resort to complicated experimental set-ups to simulate the space environment. This paper presents the theoretical development of the DEM concept, demonstrates the dynamic and kinematic equivalence, discusses the effect of model uncertainty with respect to the mapping, and presents simulation results to illustrate the equivalence in both open-loop and close-loop controls.

1 Introduction

Space robots offer potential benefits for future space exploration [11]. Their use minimize the risks associated with extra-vehicular activities (EVA's) and enable astronauts to dedicate their attention to primary rather than secondary activities, which can be delegated to a group of robots. There is a drawback, however, to the use of robots aboard spacecrafts, namely, the nonholonomic nature of the combined manipulator and free-floating base system (henceforth denoted Space Manipulator System, or SM for short) [5]. The nonholonomic characteristic of SM's prevent their widespread use in three ways: first, obtaining the dynamic model of an SM is more complicate than obtaining the model of a conventional fixed-base manipulator. Several different approaches have been proposed in the past, involving Lagrange's equations, Newton-Euler's method, Hamilton's equations, the use of barycenters, and the Virtual Manipulator (VM) method [3], [4], [7], [9], [12]. Second, SM's are subject not only to classical kinematic singularities, but also to dynamic ones [7]. Third, experiments designed to provide researchers with an understanding of how a space robot behaves and affects its base position and orientation during motion usually requires complex equipment for gravity compensation and free-flotation simulation [10], such as counterweights, buoyancy pools, Stewart platform parallel mechanisms, or air tables.

The VM is a very useful tool not only for the development of the dynamic equations of the SM, but also for the analysis of the robot's workspace. The VM is a fixed-base robot whose first joint is a passive spherical one, representing the free-floating nature of the SM's base. Its use reduces the number of dynamic equations by 3, because its definition incorporates the constraints imposed by the principle of linear momentum conservation. The VM, however, is an idealized massless kinematic chain and can only be simulated in a computer program. It cannot be mechanically built and therefore cannot be used as an experimental testbed for space manipulators. Having noted this, we propose in this paper the concept of the Dynamically Equivalent Manipulator, or DEM for short. The DEM goes beyond the VM concept, in that it represents the SM both kinematically and dynamically. The DEM is a real fixed-base robot which can be physically built and experimentally used for studying the dynamic behavior of the SM. The dynamics of the DEM under the action of any given control law map identically to the dynamics of the SM; therefore, a deep understanding of the behavior of a space robot and its base can be obtained through experiments with a conventional fixed-base robot. Besides experimental evaluation, the DEM can be used as a tool for the development of the dynamic model of the SM. The dynamic equations of the two systems are identical, but obtaining them via the DEM amounts to simply writing down

the equations of a fixed-base robot. These are simple, very well understood, and several computer programs are available for this purpose.

In this paper, we will develop the dynamic models of the SM and those of a fixed-base manipulator with a passive, spherical joint at the base. Comparing these models we obtain the conditions for kinematic and dynamic equivalence between the DEM and the SM. This equivalence is valid not only for free-floating SM's, whose base attitude is not controlled, but also for the case where the base attitude is actively controlled. We demonstrate this fact by showing that the angular momentum of both systems are identical. This is the same as saying that the presence of a passive spherical joint represents the SM's conservation of angular momentum. We present a comprehensive simulation study showing the kinematic and dynamic equivalence between the SM and the DEM, both under open-loop and closed-loop control laws. Last, we investigate the effect of model uncertainty in the mapping from the SM parameters to the DEM ones, and illustrate graphically such error mapping.

2 Nomenclature

The following is the nomenclature we will use throughout the paper, unless otherwise noted. Additional symbols will be explained following the paragraphs where they first appear. We will use left superscript numbers to indicate the frame a vector is referred to. A lack of such superscript indicates that the vector is written with respect to the coordinate frame fixed on the respective body.

$R(k, \alpha)$ = rotation matrix describing a rotation of α around axis k

R^i_j = the rotation matrix that describes the coordinate frame j relative to frame i

$\mathbf{z}, z$ = boldface letters represent vectors; the same letter, in non-boldface type, represents the vector's magnitude

0 = coordinate frame attached to the SM's total center of mass

$1, \ldots, n+1$ = coordinates frames respectively attached to the center of mass of the SM's 1st, ..., $(n+1)$-th link

C_0 = SM's total center of mass

C_i = center of mass of the SM's i-th link

J_i = joint connecting the SM's $(i-1)$-th and i-th links

θ_i = the relative rotation of the SM's $(i+1)$-th link around joint J_{i+1}

(ϕ, θ, ψ) = Z-Y-Z Euler angles representing the orientation of the SM's base (link 1)

ρ_i = vector connecting C_0 and C_i written *with respect to the inertial frame*

$\dot{\rho}_i$ = inertial linear velocity of C_i

ω_i = angular velocity of C_i

$$\omega_1 = \begin{bmatrix} 0 & -\sin\phi & \cos\phi\sin\theta \\ 0 & \cos\phi & \sin\phi\sin\theta \\ 1 & 0 & \cos\theta \end{bmatrix} \begin{bmatrix} \dot{\phi} \\ \dot{\theta} \\ \dot{\psi} \end{bmatrix} = B_s \begin{bmatrix} \dot{\phi} \\ \dot{\theta} \\ \dot{\psi} \end{bmatrix}$$

$\mathbf{u}_i$ = the axis of rotation of joint J_i with respect to frame i

${}^0\mathbf{u}_i = R_i^0 \mathbf{u}_i$

$\mathbf{v}_1$ = the unit vector in the direction from C_1 to joint J_2 with respect to frame 1

$\mathbf{v}_{n+1}$ = the unit vector in the direction from joint J_n to the center of mass of the SM's $(n+1)$-th link with respect to frame $n+1$

$\mathbf{v}_i$ = the unit vector in the direction from joint J_i to joint J_{i+1} with respect to frame i

${}^0\mathbf{v}_i = R_i^0 \mathbf{v}_i$

$\mathbf{R}_i$ = vector connecting C_i to J_{i+1}

$\mathbf{L}_i$ = vector connecting J_i to C_i

m_i, $\mathbf{I}_i$ = mass and inertia tensor of the SM's i-th link

$M_t = m_1 + \ldots + m_{n+1}$ = SM's total mass

T = SM's kinetic energy

L = SM's Lagrangian

$1', \ldots, (n+1)'$ = coordinates frames respectively attached to the center of mass of the DEM 1st, ..., $(n+1)$-th link

C_i' = center of mass of the DEM's i-th link

J_i' = joint connecting the DEM's $(i-1)$-th and i-th links

θ_i' = the relative rotation of the DEM's i-th link around joint J_i'

(ϕ', θ', ψ') = Z-Y-Z Euler angles representing the orientation of the DEM's first joint

v_{ci}' = inertial linear velocity of C_i'

ω_i' = angular velocity of C_i'

$$\omega_1' = \begin{bmatrix} 0 & -\sin\phi' & \cos\phi'\sin\theta' \\ 0 & \cos\phi' & \sin\phi'\sin\theta' \\ 1 & 0 & \cos\theta' \end{bmatrix} \begin{bmatrix} \dot{\phi}' \\ \dot{\theta}' \\ \dot{\psi}' \end{bmatrix} = B_s' \begin{bmatrix} \dot{\phi}' \\ \dot{\theta}' \\ \dot{\psi}' \end{bmatrix}$$

$\mathbf{u}_i'$ = the axis of rotation of joint J_i' with respect to frame i'

${}^0\mathbf{u}_i' = R_{i'}^0 \mathbf{u}_i'$

$\mathbf{v}_{n+1}'$ = the unit vector in the direction from joint J_n' to the center of mass of the DEM's $(n+1)$-th link with respect to frame $(n+1)'$

$\mathbf{v}_i'$ = the unit vector in the direction from joint J_i' to joint J_{i+1}' with respect to frame i'

${}^0\mathbf{v}_i' = R_{i'}^0 \mathbf{v}_i'$

$\mathbf{W}_i$ = vector connecting J_i' to J_{i+1}'

$\mathbf{l}_{ci}$ = vector connecting J_i' to C_i'

m_i', $\mathbf{I}_i'$ = mass and inertia tensor of the DEM's i-th link

T' = DEM's kinetic energy

L' = DEM's Lagrangian

3 Dynamic model of a free-floating space manipulator system

Consider an n-link serial-chain rigid manipulator mounted on a free-floating base, as shown in Figure 1. The combination of both the manipulator and its base forms the so-called *space manipulator system*, or SM, with $n+1$ rigid bodies connected by n revolute joints. We will denote the base of the SM as link 1, the links of the manipulator as links 2 through $n+1$, and the joint connecting links $i-1$ and i as joint J_i. We assume that no external forces and torques act on the SM. Consequently, its center of mass C_0 remains fixed in inertial space and can be selected as the origin of the inertial coordinate frame (frame 0 in Figure 2). Frames $1, \ldots,$ and $n+1$ are the coordinate frames attached to each of the links' center of mass.

The Lagrangian of a free-floating space manipulator system is equal to its kinetic energy, since it is assumed that the system does not have elastic components and is not acted upon by gravitational forces. Adopting $\mathbf{q} = \begin{bmatrix} \phi & \theta & \psi & \theta_1 & \cdots & \theta_n \end{bmatrix}^T = \begin{bmatrix} q_1 & \cdots & q_{n+3} \end{bmatrix}^T$ as the vector of generalized coordinates, Lagrange's equation can be written as:

$$\frac{d}{dt}\left(\frac{\partial T}{\partial \dot{q}_i}\right) - \frac{\partial T}{\partial q_i} = Q_i, \qquad i = 1, \ldots, n+3, \tag{1}$$

where Q_i is the generalized force corresponding to the generalized coordinate q_i:

$$\begin{array}{rcll} Q_i & = & 0, & i = 1, 2, 3, \\ Q_i & = & \tau_{i-3}, & i = 4, \ldots, n+3, \end{array} \tag{2}$$

and τ_i is the torque exerted on the i-th joint.

To obtain an expression for the SM's kinetic energy we must find the expressions of the linear and angular velocities of each link with respect to the inertial frame, as a function of the generalized coordinates $\mathbf{q}$. We use the Virtual Manipulator method [9] to obtain these quantities. Let $\mathbf{H}_i$ be the Virtual Manipulator whose end point is the center of mass of the i-th link. It is defined as:

$$\mathbf{H}_i = \begin{bmatrix} \mathbf{H}_i(1) \\ \mathbf{H}_i(2) \\ \cdots \\ \mathbf{H}_i(n+1) \end{bmatrix} = \begin{bmatrix} {}^0\mathbf{v}_1 H_i(1) \\ {}^0\mathbf{v}_2 H_i(2) \\ \cdots \\ {}^0\mathbf{v}_{n+1} H_i(n+1) \end{bmatrix}, \tag{3}$$

where $H_i(j) = \|\mathbf{H}_i(j)\|$ and each component of $\mathbf{H}_i$ is defined as:

$$\begin{array}{rcll} \mathbf{H}_i(1) & = & \mathbf{r}_1, & \\ \mathbf{H}_i(j) & = & \mathbf{r}_j + \mathbf{l}_j, & 1 < j < i, \\ \mathbf{H}_i(j) & = & \mathbf{r}_i + \mathbf{l}_i - \mathbf{R}_i, & j = i, \\ \mathbf{H}_i(j) & = & \mathbf{r}_j + \mathbf{l}_j - \mathbf{R}_j - \mathbf{L}_j, & j > i, \end{array} \tag{4}$$

with

$$\mathbf{r}_i = \mathbf{R}_i \sum_{k=1}^{i} m_k / M_t, \tag{5}$$

$$\mathbf{l}_i = \mathbf{L}_i \sum_{k=1}^{i-1} m_k / M_t. \tag{6}$$

The translational velocity of the center of mass of the i-th link can be written as:

$$\begin{array}{rcl} \dot{\rho}_i & = & \left[\begin{array}{cccc} \omega_1 \times & \omega_2 \times & \cdots & \omega_{n+1} \times \end{array} \right] \mathbf{H}_i \\ & = & \left[\begin{array}{cccc} -\mathbf{H}_i(1) \times & -\mathbf{H}_i(2) \times & \cdots & -\mathbf{H}_i(n+1) \times \end{array} \right] \omega \\ & = & J_{vi}(\mathbf{H}_i, \boldsymbol{q}) \dot{\mathbf{q}}. \end{array} \tag{7}$$

where $[\omega_i \times]$ represents the 3×3 skew-symmetric matrix obtained from the elements of the vector ω_i. The angular velocities of the SM's links, ω_i, are stacked to form the vector ω, the

angular velocity of the SM:

$$\begin{aligned}
\omega &= \begin{bmatrix} \omega_1^T & \omega_2^T & \cdots & \omega_{n+1}^T \end{bmatrix}^T \\
&= \begin{bmatrix} B_s & \mathbf{0} & 0 & \cdots & 0 \\ B_s & {}^0\mathbf{u}_2 & \mathbf{0} & \cdots & 0 \\ B_s & {}^0\mathbf{u}_2 & {}^0\mathbf{u}_3 & \cdots & 0 \\ \vdots & \vdots & \vdots & \cdots & \vdots \\ B_s & {}^0\mathbf{u}_2 & {}^0\mathbf{u}_3 & \cdots & {}^0\mathbf{u}_{n+1} \end{bmatrix} \begin{bmatrix} \dot{q}_1 \\ \dot{q}_2 \\ \dot{q}_3 \\ \vdots \\ \dot{q}_{n+3} \end{bmatrix} \\
&= \begin{bmatrix} B_s & 0 & 0 & \cdots & 0 \\ B_s & R_2^0\mathbf{u}_2 & 0 & \cdots & \mathbf{0} \\ B_s & R_2^0\mathbf{u}_2 & R_3^0\mathbf{u}_3 & \cdots & \mathbf{0} \\ \vdots & \vdots & \vdots & \cdots & \vdots \\ B_s & R_2^0\mathbf{u}_2 & R_3^0\mathbf{u}_3 & \cdots & R_{n+1}^0\mathbf{u}_{n+1} \end{bmatrix} \begin{bmatrix} \dot{q}_1 \\ \dot{q}_2 \\ \dot{q}_3 \\ \vdots \\ \dot{q}_{n+3} \end{bmatrix} \\
&= B_\omega \dot{\mathbf{q}}. \qquad (8)
\end{aligned}$$

Then

$$\begin{aligned}
\omega_i &= \begin{bmatrix} B_s & R_2^0\mathbf{u}_2 & R_3^0\mathbf{u}_3 & \cdots & R_i^0\mathbf{u}_i & \mathbf{0} & \cdots & 0 \end{bmatrix} \begin{bmatrix} \dot{q}_1 \\ \dot{q}_2 \\ \dot{q}_3 \\ \vdots \\ \dot{q}_{n+3} \end{bmatrix} \\
&= B_{\omega i} \dot{\mathbf{q}}. \qquad (9)
\end{aligned}$$

The total kinetic energy of the SM system is then

$$\begin{aligned}
T &= \sum_{i=1}^{n+1} \left(\frac{1}{2} m_i \dot{\rho}_i^T \dot{\rho}_i + \frac{1}{2} \omega_i^T R_i^0 \mathbf{I}_i R_i^{0T} \omega_i \right) \\
&= \frac{1}{2} \dot{\mathbf{q}}^T M \dot{\mathbf{q}}, \qquad (10)
\end{aligned}$$

where

$$M = \sum_{i=1}^{n+1} \left(m_i J_{vi}^T J_{vi} + B_{\omega i}^T R_i^0 \mathbf{I}_i R_i^{0T} B_{\omega i} \right). \qquad (11)$$

Substitution of (10) into (1) yields the desired dynamic equations of the space manipulator system.

4 Dynamic model of a fixed-base manipulator with a passive spherical joint

In this section we will develop the dynamic model of an $(n+1)$-link fixed-base robot manipulator whose first joint is a passive spherical one. In the next section we will compare this model to the SM's obtained previously to propose the equivalence between the DEM and the SM.

We attach the frames $1',\ldots,(n+1)'$ to the center of mass of each link of the manipulator (Figure 3). The vector of generalized coordinates is $\mathbf{q}' = \begin{bmatrix} \phi' & \theta' & \psi' & \theta_1' & \cdots & \theta_n' \end{bmatrix}^T = \begin{bmatrix} q_1' & \cdots & q_{n+3}' \end{bmatrix}^T$. Similarly to derivation for the SM, we can write

$$\begin{aligned} \omega' &= \begin{bmatrix} \omega_1' & \omega_2' & \cdots & \omega_{n+1}' \end{bmatrix}^T \\ &= \begin{bmatrix} B_s' & \mathbf{0} & 0 & \cdots & 0 \\ B_s' & {}^0\mathbf{u}_2' & 0 & \cdots & 0 \\ B_s' & {}^0\mathbf{u}_2' & {}^0\mathbf{u}_3' & \cdots & \mathbf{0} \\ \vdots & \vdots & \vdots & \cdots & \vdots \\ B_s' & {}^0\mathbf{u}_2' & {}^0\mathbf{u}_3' & \cdots & {}^0\mathbf{u}_{n+1}' \end{bmatrix} \begin{bmatrix} \dot{q}_1' \\ \dot{q}_2' \\ \dot{q}_3' \\ \vdots \\ \dot{q}_{n+3}' \end{bmatrix} \\ &= B_\omega' \dot{\mathbf{q}}', \end{aligned} \tag{12}$$

and

$$\omega_i' = B_{\omega i}' \dot{\mathbf{q}}'. \tag{13}$$

Let $\mathbf{H}_i'$ be the vector defined as

$$\mathbf{H}_i' = \begin{bmatrix} \mathbf{H}_i'(1) \\ \mathbf{H}_i'(2) \\ \cdots \\ \mathbf{H}_i'(n+1) \end{bmatrix} = \begin{bmatrix} {}^0\mathbf{v}_1' H_i'(1) \\ {}^0\mathbf{v}_2' H_i'(2) \\ \cdots \\ {}^0\mathbf{v}_{n+1}' H_i'(n+1) \end{bmatrix}, \tag{14}$$

where $H_i'(j) = \|\mathbf{H}_i'(j)\|$ and the components of $\mathbf{H}_i'$ are given by

$$\mathbf{H}_i'(j) = \begin{cases} \mathbf{W}_j, & 1 \leq j < i, \\ \mathbf{l}_{cj}, & j = i, \\ [0 \;\; 0 \;\; 0]^T, & j > i. \end{cases} \tag{15}$$

The linear velocity of the center of mass of the i-th link is given by:

$$\begin{aligned} v_{ci}' &= \begin{bmatrix} \omega_1' \times & \omega_2' \times & \cdots & \omega_{n+1}' \times \end{bmatrix} \mathbf{H}_i' \\ &= \begin{bmatrix} -\mathbf{H}_i'(1) \times & -\mathbf{H}_i'(2) \times & \cdots & -\mathbf{H}_i'(n+1) \times \end{bmatrix} \omega' \\ &= J_{vi}'(\mathbf{H}_i', \mathbf{q}') \dot{\mathbf{q}}'. \end{aligned} \tag{16}$$

We assume that the manipulator operates in the same environment as does the SM, i.e., in the absence of gravity; consequently, the potential energy of the system is equal to zero and the Lagrangian is equal to the kinetic energy:

$$\begin{aligned} L' = T' &= \sum_{i=1}^{n+1} \left(\frac{1}{2} m_i' v_{ci}'^T v_{ci}' + \frac{1}{2} \omega_i'^T R_{i'}^0 \mathbf{I}_i' R_{i'}^{0\,T} \omega_i' \right) \\ &= \frac{1}{2} \dot{\mathbf{q}}'^T M' \dot{\mathbf{q}}'. \end{aligned} \tag{17}$$

So far we have obtained the expressions of the Lagrangian of the SM, and that of the fixed-base manipulator with a passive, spherical joint. In the next section we study their relationship and the conditions under which they are equivalent.

5 The DEM and its equivalence to the SM

5.1 Definition of Dynamically Equivalent Manipulator

Definition: The Dynamically Equivalent Manipulator (DEM for short) is a fixed-base manipulator whose first joint is a passive spherical one, and whose kinematic and dynamic models are identical to those of a given space manipulator system. The parameters of the DEM satisfy the following algebraic equations:

$$\begin{aligned} m_i' &= \frac{M_i^2 m_i}{\sum_{k=1}^{i-1} m_k \sum_{k=1}^{i} m_k}, && i = 2, \ldots, n+1, \\ \mathbf{I}_i' &= \mathbf{I}_i, && i = 1, \ldots, n+1, \\ \mathbf{W}_1 &= \mathbf{r}_1, \\ \mathbf{W}_i &= \mathbf{r}_i + \mathbf{l}_i, && i = 2, \ldots, n+1. \\ \mathbf{l}_{c1} &= \mathbf{0}, \\ \mathbf{l}_{ci} &= \frac{\sum_{k=1}^{i-1} m_k}{M_t} \mathbf{L}_i, && i = 2, \ldots, n+1. \end{aligned} \tag{18}$$

The vectors $\mathbf{W}_i$ represent the DEM link lengths and their inertial orientations with respect to the SM's inertial frame; m_i' is the mass the DEM's i-th link; $\mathbf{I}_i' \in R^{3\times 3}$ is the inertia tensor the DEM's i-th link; and $\mathbf{l}_{ci}$ is the vector from the DEM's i-th joint to the center of mass of the i-th link.

Remark 1: As it will be seen in the sequence, the dynamic equivalence between the SM and the DEM does not depend on the value of m_1'.

Remark 2: Not surprisingly, the DEM's links' length and orientation were chosen identical to those of the SM's Virtual Manipulator. This choice will be clear in the next subsection when we address the kinematic equivalence between the SM and the DEM.

Note that, without loss of generality, we assume that the center of mass of the SM's i-th link ($i = 2, \ldots, n$) lies on the line connecting the SM's i-th and $(i+1)$-th joints.

5.2 Kinematic equivalence between the SM and the DEM

The DEM is shown in Figure 4. Its coordinate frames are parallel to the corresponding frames of the SM, and its base coincides with the total center of mass of the SM. Consequently, the DEM is geometrically identical to the end-effector Virtual Manipulator of the SM [9] and it inherits all the nice properties of the Virtual Manipulator, namely:

1. The axis of the i-th DEM joint, ${}^0\mathbf{u}_i'$, is always parallel to the axis of the i-th SM joint, ${}^0\mathbf{u}_i$.

2. The displacement of each of the DEM's joints during motion is identical to the displacement of the corresponding SM joint.

3. The DEM *end point* will always coincide with the SM's manipulator end effector.

Mathematically, we can write:

$$\begin{aligned} \mathbf{q} &= \mathbf{q}', \\ \omega &= \omega', \\ R_i^0 &= R_{i'}^0, \\ {}^0\mathbf{u}_i &= {}^0\mathbf{u}_i', \\ {}^0\mathbf{v}_i &= {}^0\mathbf{v}_i', \\ J_{v,n+1} &= J_{v,n+1}'. \end{aligned} \tag{19}$$

5.3 Dynamic equivalence between the SM and the DEM

To establish the dynamic equivalence between the DEM and the SM, we will separately study the contributions of the linear and angular components of the kinetic energy to the systems' Lagrangian. From (19) and the fact that $\mathbf{I}_i' = \mathbf{I}_i$, we can immediately conclude that the angular components are identical. It rests then to consider the linear component of the kinetic energies, T_l and T_l'.

We start by presenting the following lemma.

Lemma 1:

$$\sum_{i=1}^{n+1} m_i H_i(j) = 0, \qquad j = 1, \ldots, n+1.$$

Proof: Recall that the center of mass of the SM's i-th link lies on the line supported by

the i-th and $(i+1)$-th joints. Therefore, the vectors $\mathbf{r}_i$, $\mathbf{l}_i$, $\mathbf{R}_i$, and $\mathbf{L_i}$ are all collinear, and the norm of $\mathbf{H}_i$ in (4), denoted H_i, is equal to the sum of the magnitudes of the individual components in the summations. We can therefore write:

$$\begin{aligned}\sum_{i=1}^{n+1} m_i H_i(j) &= \sum_{i=1}^{j-1} m_i(r_j + l_j - R_j - L_j) + m_j(r_j + l_j - R_j) \\ &\quad + \sum_{i=j+1}^{n+1} m_i(r_j + l_j) \\ &= M_i r_j - \sum_{i=1}^{j} m_i R_j + M_i l_j - \sum_{i=1}^{j-1} m_i L_j. \end{aligned} \tag{20}$$

Substituting (5) and (6) in the above equation we get the desired result.

The linear velocity of the center of mass of the SM's i-th link, $\dot{\rho}_i$, can be written as:

$$\begin{aligned}\dot{\rho}_i &= \left[\begin{array}{cccc} \omega_1\times & \omega_2\times & \cdots & \omega_{n+1}\times \end{array}\right]\mathbf{H}_i \\ &= \left[\begin{array}{cccc} (\omega_1\times)^0\mathbf{v_1} & (\omega_2\times)^0\mathbf{v}_2 & \cdots & (\omega_{n+1}\times)^0\mathbf{v}_{n+1} \end{array}\right]H_i \\ &= \left[\begin{array}{cccc} (\omega_1\times)R_1^0\mathbf{v}_1 & (\omega_2\times)R_2^0\mathbf{v}_2 & \cdots & (\omega_{n+1}\times)R_{n+1}^0\mathbf{v}_{n+1} \end{array}\right]H_i \\ &= J_h H_i. \end{aligned} \tag{21}$$

Then

$$\begin{aligned}\dot{\rho}_i^T\dot{\rho}_i &= [J_h H_i]^T J_h H_i \\ &= \left[\begin{array}{ccc} H_i^T J_{h1}^T & H_i^T J_{h2}^T & H_i^T J_{h3}^T \end{array}\right]\left[\begin{array}{c} J_{h1}H_i \\ J_{h2}H_i \\ J_{h3}H_i \end{array}\right] \\ &= \sum_{k=1}^{3} J_{hk} H_i H_i^T J_{hk}^T, \end{aligned} \tag{22}$$

where $J_{hk}H_i = H_i^T J_{hk}^T$, since $J_{hk}H_i$ is a scalar. The linear component of the SM's kinetic energy is then given by:

$$\begin{aligned}T_l &= \sum_{i=1}^{n+1}\frac{1}{2}m_i\dot{\rho}_i^T\dot{\rho}_i \\ &= \frac{1}{2}\sum_{i=1}^{n+1} m_i \sum_{k=1}^{3} J_{hk}H_i H_i^T J_{hk}^T \\ &= \frac{1}{2}\sum_{k=1}^{3} J_{hk}E_l J_{hk}^T, \end{aligned} \tag{23}$$

where

$$E_l = \sum_{i=1}^{n+1} m_i H_i H_i^T \tag{24}$$

is a symmetric matrix whose (j,k) element is given by:

$$\begin{aligned} E_l(j,k) &= \sum_{i=1}^{n+1} m_i H_i(j) H_i(k) \\ &= \sum_{i=1}^{k-1} m_i H_i(j)(r_k + l_k - R_k - L_k) + m_k H_k(j)(r_k + l_k - R_k) \\ &\quad + \sum_{i=k+1}^{n+1} m_i H_i(j)(r_k + l_k) \\ &= \sum_{i=1}^{n+1} m_i H_i(j)(r_k + l_k) + m_k H_k(j) L_k + \sum_{i=k+1}^{n+1} m_i H_i(j)(R_k + L_k). \end{aligned} \tag{25}$$

Because $\sum_{i=1}^{n+1} m_i H_i(j) = 0$ (Lemma 1), we can simplify the above equation to:

$$E_l(j,k) = m_k H_k(j) L_k + \sum_{i=k+1}^{n+1} m_i H_i(j)(R_k + L_k). \tag{26}$$

When $i > j$, $H_i(j) = r_j + l_j = H_{n+1}(j)$. Therefore,

$$E_l(j,k) = [m_k L_k + \sum_{i=k+1}^{n+1} m_i (R_k + L_k)] H_{n+1}(j), \tag{27}$$

$$\begin{aligned} E_l(k,k) &= m_k H_k(k) L_k + \sum_{i=k+1}^{n+1} m_i H_i(k)(R_k + L_k) \\ &= m_k L_k (H_{n+1}(k) - R_k) + \sum_{i=k+1}^{n+1} m_i H_i(k)(R_k + L_k) \\ &= -m_k L_k R_k + \sum_{i=k}^{n+1} m_i H_{n+1}(k) L_k + \sum_{i=k+1}^{n+1} m_i H_{n+1}(k) R_k. \end{aligned} \tag{28}$$

We now repeat the above steps for the DEM. The linear velocity of the center of mass of the i-th link, v_{ci}', can be written as:

$$\begin{aligned} v_{ci}' &= \left[\begin{array}{cccc} \omega_1' \times & \omega_2' \times & \cdots & \omega_n' \times \end{array} \right] \mathbf{H}_i' \\ &= \left[\begin{array}{cccc} (\omega_1' \times)^0 \mathbf{v}_1' & (\omega_2' \times)^0 \mathbf{v}_2' & \cdots & (\omega_n' \times)^0 \mathbf{v}_{n+1}' \end{array} \right] H_i' \\ &= \left[\begin{array}{cccc} (\omega_1' \times) R_1^0 \mathbf{v}_1' & (\omega_2' \times) R_2^0 \mathbf{v}_2' & \cdots & (\omega_n' \times) R_{n+1}^0 \mathbf{v}_{n+1'} \end{array} \right] H_i' \\ &= J_h' H_i'. \end{aligned} \tag{29}$$

Recall that the kinematic properties of the DEM are identical to those of the SM; consequently, $J_h' = J_h$ and:

$$v_{ci}'^T v_{ci}' = [J_h H_i']^T J_h H_i'$$

$$= \begin{bmatrix} H_i'^T J_{k1}^T & H_i'^T J_{k2}^T & H_i'^T J_{k3}^T \end{bmatrix} \begin{bmatrix} J_{k1} H_i' \\ J_{k2} H_i' \\ J_{k3} H_i' \end{bmatrix}$$

$$= \sum_{k=1}^{3} J_{kk} H_i' H_i'^T J_{kk}^T. \tag{30}$$

The DEM's translational kinetic energy is expressed as

$$\begin{aligned} T_l' &= \sum_{i=1}^{n+1} \frac{1}{2} m_i' v_{ci}'^T v_{ci}' \\ &= \frac{1}{2} \sum_{i=1}^{n+1} m_i' \sum_{k=1}^{3} J_{kk} H_i' H_i'^T J_{kk}^T \\ &= \frac{1}{2} \sum_{k=1}^{3} J_{kk} E_l' J_{kk}^T, \end{aligned} \tag{31}$$

where

$$E_l' = \sum_{i=1}^{n+1} m_i' H_i' H_i'^T \tag{32}$$

is a symmetric matrix.

From (4) and (15) we can write:

$$H_{n+1}'(k) = H_{n+1}(k), \qquad k = 1, \ldots, n+1. \tag{33}$$

Therefore,

$$E_l'(j,k) = [m_k' l_{ck} + \sum_{i=k+1}^{n+1} m_i' H_{n+1}(k)] H_{n+1}(j), \tag{34}$$

$$\begin{aligned} E_l'(k,k) &= m_k' l_{ck}^2 + \sum_{i=k+1}^{n+1} m_i' (H_i'(k))^2 \\ &= m_k' l_{ck}^2 + \sum_{i=k+1}^{n+1} m_i' (H_{n+1}(k))^2. \end{aligned} \tag{35}$$

We now assume that $E_l = E_l'$, or, equivalently, that $T_l = T_l'$ and that the SM and the DEM are dynamically identical. We will show that the definitions of the DEM parameters as in (18) form a set of sufficient conditions for this assumption to be true. The proof is by induction from link $n+1$ to link 2, with link 1 being treated as a special case. When $i = n+1$,

$$E_l(i,i) = E_l(n+1, n+1) = m_{n+1} (H_{n+1}(n+1))^2 \tag{36}$$

$$E_l(j,i) = E_l(j,n+1) = m_{n+1} H_{n+1}(j) L_{n+1} \tag{37}$$

$$E_l^{'}(i,i) = E_l^{'}(n+1,n+1) = m_{n+1}^{'} l_{c,n+1}^2 \tag{38}$$

$$E_l^{'}(j,i) = E_l^{'}(j,n+1) = m_{n+1}^{'} l_{c,n+1} H_{n+1}(j) \tag{39}$$

Since we assumed that $E_l = E_l^{'}$, we compare the above expressions and obtain:

$$l_{c,n+1} = \frac{\sum_{k=1}^{n} m_k}{M_t} L_{n+1}, \tag{40}$$

$$m_{n+1}^{'} = \frac{M_t m_{n+1}}{\sum_{k=1}^{n} m_i}. \tag{41}$$

Now take $i > k$ $(k \geq 2)$, and assume that

$$l_{ci} = \frac{\sum_{k=1}^{i-1} m_k}{M_t} L_i, \tag{42}$$

$$m_i^{'} = \frac{M_t^2 m_i}{\sum_{k=1}^{i-1} m_k \sum_{k=1}^{i} m_k}. \tag{43}$$

For $k \geq 2$ we can compare the (j,k) elements of E_l and $E_l^{'}$ and write:

$$\begin{aligned} m_k^{'} l_{ck} &= m_k L_k + \sum_{i=k+1}^{n+1} m_i (R_k + L_k) - \sum_{i=k+1}^{n+1} m_i^{'} H_{n+1}(k) \\ &= m_k L_k \frac{M_t}{\sum_{i=1}^{k} m_i}. \end{aligned} \tag{44}$$

Also, for the k-th diagonal element we can write:

$$\begin{aligned} m_k^{'} l_{ck}^2 &= -m_k L_k R_k + \sum_{i=k}^{n+1} m_i H_{n+1}(k) L_k + \sum_{i=k+1}^{n+1} m_i H_{n+1}(k) R_k - \sum_{i=k+1}^{n+1} m_i^{'} (H_{n+1}(k))^2 \\ &= m_k L_k^2 \frac{\sum_{i=1}^{k-1} m_i}{\sum_{i=1}^{k} m_i}, \end{aligned} \tag{45}$$

Because masses are positive quantities we can divide (45) by (44), which results in:

$$l_{ck} = \frac{\sum_{i=1}^{k-1} m_i}{M_t} L_k. \tag{46}$$

Substituting (46) back into (44) we obtain:

$$m_k' = \frac{M_t^2 m_k}{\sum_{i=1}^{k-1} m_i \sum_{i=1}^{k} m_i}. \tag{47}$$

Finally, for the special case $k = 1$, we can write $E_l(1,1) = E_l'(1,1)$, or, equivalently,

$$m_1' l_{c1}^2 = 0 \tag{48}$$

Because $m_1' \neq 0$, it must be $l_{c1} = 0$. Therefore the dynamic equivalence does not depend on the value of m_1', and the mass of the DEM's first link can be assigned arbitrarily.

At first sight it might be striking that we can assign the value of m_1' arbitrarily. The explanation is as follows. To obtain the $2(n+1)$ values m_i' and l_{ci} we compared the (identical) matrices E_l and E_l'. Because these matrices are symmetric, we only have to compare the $(n+1)(n+2)/2$ elements at and above the main diagonal. But the elements at any column, excluding the ones at the diagonal, are not independent. In fact, every element $E_l(j,k)$, $j \neq k$, is proportional to $E_l(1,k)$. Consequently, we only have to compare the $n+1$ diagonal elements and the n elements $E_l(1,k)$, for a total of $2n+1$ independent elements. Therefore, when we equate E_l to E_l' we end up with one more unknown than equations, and we can set this unknown (which is m_1') arbitrarily.

Summarizing, we showed that both the linear and angular components of the kinetic energies of the SM and DEM are identical. This is the same as showing that their Lagrangians are identical, since both are rigid and operate in a zero-gravity environment. Because the generalized forces acting on both are assumed to be identical, we can conclude that the dynamics of the SM and that of the DEM are the same.

5.4 Mapping a DEM to a SM

We now present the inverse mapping problem, i.e., the problem of computing the kinematic and dynamic parameters of the SM given those of the DEM. Solving equations (18) we obtain:

$$
\begin{aligned}
m_1 &= \frac{M_t^2}{M_t + \sum_{k=2}^{n+1} m_k'}, \\
m_i &= \frac{M_t^2 m_i'}{\left(M_t + \sum_{k=i}^{n+1} m_k'\right)\left(M_t + \sum_{k=i+1}^{n+1} m_k'\right)}, \quad i = 2, \ldots, n+1, \\
m_{n+1} &= \frac{M_t m_{n+1}'}{M_t + m_{n+1}'} \\
\mathbf{I}_i &= \mathbf{I}_i' \qquad\qquad\qquad\qquad\qquad\qquad i = 1, \ldots, n-1, \\
\mathbf{R}_i &= (\mathbf{W}_i - \mathbf{l}_{ci}) \frac{M_t + \sum_{k=i+1}^{n+1} m_k'}{M_t}, \qquad i = 1, \ldots, n, \\
\mathbf{R}_{n+1} &= (\mathbf{W}_i - \mathbf{l}_{ci}), \\
\mathbf{L}_i &= \mathbf{l}_{ci} \frac{M_t + \sum_{k=i}^{n+1} m_k'}{M_t}, \qquad\qquad i = 2, \ldots, n+1.
\end{aligned}
\tag{49}
$$

Note that the set of equations (49) does not uniquely determine the mass properties of the SM. The solution is unique, however, when either the SM's total mass or the mass of each link is specified.

6 Angular momentum

We have so far demonstrated that the proposed DEM is equivalent to a free-floating SM (i.e., a SM whose attitude is not controlled). In this section we demonstrate that the DEM is also a valid concept when the SM is free-flying, i.e., when the SM base attitude is controlled via reaction wheels. This amounts to showing that the angular momentum of the DEM is identical to that of the SM.

Using the VM concept we can express the position of the center of mass of the SM's i-th link as:

$$
\begin{aligned}
\rho_i &= \left[\begin{array}{cccc} R_1^0 \mathbf{v}_1 & R_2^0 \mathbf{v}_2 & \cdots & R_{n+1}^0 \mathbf{v}_{n+1} \end{array} \right] H_i \\
&= G H_i.
\end{aligned}
\tag{50}
$$

We can thus express the velocity of the center of mass as:

$$
\dot{\rho}_i = \left[\begin{array}{cccc} \frac{\partial G}{\partial q_1} H_i & \frac{\partial G}{\partial q_2} H_i & \cdots & \frac{\partial G}{\partial q_{n+3}} H_i \end{array} \right] \dot{\mathbf{q}} = D \dot{\mathbf{q}}.
\tag{51}
$$

The angular momentum of the SM is equal to:

$$
H_A = \sum_{i=1}^{n+1} \rho_i \times m_i \dot{\rho}_i + {}^0\mathbf{I}_i \omega_i
$$

$$
\begin{aligned}
&= \left(\sum_{i=1}^{n+1} GH_i \times m_i \left[\begin{array}{cccc} \frac{\partial G}{\partial q_1} H_i & \frac{\partial G}{\partial q_2} H_i & \cdots & \frac{\partial G}{\partial q_{n+3}} H_i \end{array} \right] + \sum_{i=1}^{n+1} R_i^0 \mathbf{I}_i R_i^{0T} B_{\omega i}^T \right) \dot{\mathbf{q}} \\
&= A\dot{\mathbf{q}}. \qquad (52)
\end{aligned}
$$

Using (51), we can express the SM's kinetic energy as:

$$
\begin{aligned}
T &= \sum_{i=1}^{n+1} \frac{1}{2} m_i \dot{\rho}_i^T \dot{\rho}_i + \frac{1}{2} \omega_i^T R_i^0 \mathbf{I}_i R_i^{0T} \omega_i \\
&= \frac{1}{2} \dot{\mathbf{q}}^T \sum_{i=1}^{n+1} \left(D^T m_i D + B_{\omega i}^T R_i^0 \mathbf{I}_i R_i^{0T} B_{\omega i}^T \right) \dot{\mathbf{q}} \\
&= \frac{1}{2} \dot{\mathbf{q}}^T M \dot{\mathbf{q}}. \qquad (53)
\end{aligned}
$$

Let M_u be a matrix formed by the first three rows of the inertia matrix M:

$$
\begin{aligned}
M_u &= \sum_{i=1}^{n+1} \left[\begin{array}{ccc} \frac{\partial G}{\partial q_1} H_i & \frac{\partial G}{\partial q_2} H_i & \frac{\partial G}{\partial q_3} H_i \end{array} \right]^T m_i \left[\begin{array}{cccc} \frac{\partial G}{\partial q_1} H_i & \frac{\partial G}{\partial q_2} H_i & \cdots & \frac{\partial G}{\partial q_{n+3}} H_i \end{array} \right] \\
&\quad + B_s^T \sum_{i=1}^{n+1} R_i^0 \mathbf{I}_i R_i^{0T} B_{\omega i}^T. \qquad (54)
\end{aligned}
$$

At this point we invoke the following lemma, whose proof is deferred to the end of this section:

Lemma 2:

$$
\begin{aligned}
B_s^T \cdot [GH_i \times] &= \left[\begin{array}{ccc} \frac{\partial G}{\partial q_1} H_i & \frac{\partial G}{\partial q_2} H_i & \frac{\partial G}{\partial q_3} H_i \end{array} \right]^T, \qquad (55) \\
B_s^{'T} \cdot [GH_i' \times] &= \left[\begin{array}{ccc} \frac{\partial G}{\partial q_1'} H_i' & \frac{\partial G}{\partial q_2'} H_i' & \frac{\partial G}{\partial q_3'} H_i' \end{array} \right]^T. \qquad (56)
\end{aligned}
$$

Using Lemma 2 we can rewrite M_u as:

$$
M_u = B_s^T A \qquad (57)
$$

Following the same steps above, we can obtain the expressions for the DEM's angular momentum and kinetic energy:

$$
\begin{aligned}
H_A' &= A' \dot{\mathbf{q}}' \qquad (58) \\
T' &= \frac{1}{2} \dot{\mathbf{q}}'^T M' \dot{\mathbf{q}}' \qquad (59)
\end{aligned}
$$

We additionally define M_u' as the matrix formed by the first three rows of M'; consequently:

$$
M_u' = B_s'^T A'. \qquad (60)
$$

Since we have shown that the SM and the DEM are kinematically and dynamically equivalent, we have that $T = T'$, $M = M'$, and $B_s = B_s'$. Therefore, $M_a = M_a'$, $A = A'$ and

$$H_A = H_A'. \tag{61}$$

In summary, we have shown that the angular momentum of the SM and of the DEM are identical. The identical momentum implies the identical dynamic behavior of the two systems under the action of the same external moment. This conclusion ensures that, when the SM's base attitude is controlled via reaction wheels, the DEM concept is still valid. In other words, the DEM is dynamically equivalent to the SM, with or without external moments applied.

We now give the proof of Lemma 2. The explicit expression for $B_s^T \cdot [GH_i\times]$ is:

$$\begin{aligned} & B_s^T \cdot [GH_i\times] \\ &= \begin{bmatrix} 0 & 0 & 1 \\ -s_1 & c_1 & 0 \\ c_1 s_2 & s_1 s_2 & c_2 \end{bmatrix} \begin{bmatrix} 0 & -G_3 H_i & G_2 H_i \\ G_3 H_i & 0 & -G_1 H_i \\ -G_2 H_i & G_1 H_i & 0 \end{bmatrix} \\ &= \begin{bmatrix} -G_2 H_i & G_1 H_i & 0 \\ c_1 G_3 H_i & s_1 G_3 H_i & -s_1 G_2 H_i - c_1 G_1 H_i \\ s_1 s_2 G_3 H_i - c_2 G_2 H_i & -c_1 s_2 G_3 H_i + c_2 G_1 H_i & c_1 s_2 G_2 H_i - s_1 s_2 G_1 H_i \end{bmatrix}, \end{aligned} \tag{62}$$

where s_i stands for $sin(q_i)$, c_i for $cos(q_i)$, and $G = \begin{bmatrix} G_1 & G_2 & G_3 \end{bmatrix}^T$.

To compute an explicit expression for the right-hand-side of the equality in Lemma 2, we first compute:

$$R_1^0 = R(z, q_1) R(y, q_2) R(z, q_3) \tag{63}$$

$$= \begin{bmatrix} c_1 c_2 c_3 - s_1 s_3 & -c_1 c_2 s_3 - s_1 c_3 & c_1 s_2 \\ s_1 c_2 c_3 + c_1 s_3 & -s_1 c_2 s_3 + c_1 c_3 & s_1 s_2 \\ -s_2 c_3 & s_2 s_3 & c_2 \end{bmatrix}, \tag{64}$$

and

$$\begin{aligned} \frac{\partial R_1^0}{\partial q_1} &= \begin{bmatrix} -s_1 c_2 c_3 - c_1 s_3 & s_1 c_2 s_3 - c_1 c_3 & -s_1 s_2 \\ c_1 c_2 c_3 - s_1 s_3 & -c_1 c_2 s_3 - s_1 c_3 & c_1 s_2 \\ 0 & 0 & 0 \end{bmatrix} \\ &= \begin{bmatrix} 0 & -1 & 0 \\ 1 & 0 & 0 \\ 0 & 0 & 0 \end{bmatrix} R_1^0, \end{aligned} \tag{65}$$

$$\frac{\partial R_1^0}{\partial q_2} = \begin{bmatrix} -c_1 s_2 c_3 & c_1 s_2 s_3 & c_1 c_2 \\ -c_1 s_2 c_3 & c_1 s_2 s_3 & c_1 c_2 \\ -c_2 c_3 & c_2 s_3 & -s_2 \end{bmatrix}$$

$$= \begin{bmatrix} 0 & 0 & c_1 \\ 0 & 0 & s_1 \\ -c_1 & -s_1 & 0 \end{bmatrix} R_1^0, \tag{66}$$

$$\frac{\partial R_1^0}{\partial q_3} = \begin{bmatrix} -c_1 c_2 s_3 - s_1 c_3 & -c_1 c_2 c_3 + s_1 s_3 & 0 \\ -s_1 c_2 s_3 + c_1 c_3 & -s_1 c_2 c_3 - c_1 s_3 & 0 \\ s_2 s_3 & s_2 c_3 & 0 \end{bmatrix}$$

$$= \begin{bmatrix} 0 & -c_2 & s_1 s_2 \\ c_2 & 0 & -c_1 s_2 \\ -s_1 s_2 & c_1 s_2 & 0 \end{bmatrix} R_1^0. \tag{67}$$

With the above equalities we can write:

$$R_1^0 = R(z, q_1) R(y, q_2) R(z, q_3)$$

$$= \begin{bmatrix} c_1 c_2 c_3 - s_1 s_3 & -c_1 c_2 s_3 - s_1 c_3 & c_1 s_2 \\ s_1 c_2 c_3 + c_1 s_3 & -s_1 c_2 s_3 + c_1 c_3 & s_1 s_2 \\ -s_2 c_3 & s_2 s_3 & c_2 \end{bmatrix}, \tag{68}$$

and

$$\frac{\partial R_1^0}{\partial q_1} = \begin{bmatrix} -s_1 c_2 c_3 - c_1 s_3 & s_1 c_2 s_3 - c_1 c_3 & -s_1 s_2 \\ c_1 c_2 c_3 - s_1 s_3 & -c_1 c_2 s_3 - s_1 c_3 & c_1 s_2 \\ 0 & 0 & 0 \end{bmatrix}$$

$$= \begin{bmatrix} 0 & -1 & 0 \\ 1 & 0 & 0 \\ 0 & 0 & 0 \end{bmatrix} R_1^0 \begin{bmatrix} R_1^1 \mathbf{v}_1 & R_2^1 \mathbf{v}_2 & \cdots & R_{n+1}^1 \mathbf{v}_{n+1} \end{bmatrix} H_i$$

$$= \begin{bmatrix} 0 & -1 & 0 \\ 1 & 0 & 0 \\ 0 & 0 & 0 \end{bmatrix} G H_i$$

$$= \begin{bmatrix} -G_2 H_i \\ G_1 H_i \\ 0 \end{bmatrix}. \tag{69}$$

Analogously, it is straightforward to obtain

$$\frac{\partial G}{\partial q_2} H_i = \begin{bmatrix} c_1 G_3 H_i \\ s_1 G_3 H_i \\ -s_1 G_2 H_i - c_1 G_1 H_i \end{bmatrix}. \tag{70}$$

$$\frac{\partial G}{\partial q_3} H_i = \begin{bmatrix} s_1 s_2 G_3 H_i - c_2 G_2 H_i \\ -c_1 s_2 G_3 H_i + c_2 G_1 H_i \\ c_1 s_2 G_2 H_i - s_1 s_2 G_1 H_i \end{bmatrix}. \tag{71}$$

From (62), (69), (70), and (71) we obtain (55) as the desired result. Analogous steps can be used to establish (56).

The reader who is familiar with the current literature on underactuated manipulators [1], [2], [6] might be puzzled by the above result. After all, the conservation of angular momentum of the SM is a constraint involving only velocities, while manipulators with passive joints are systems whose constraints involve velocities and accelerations [6]. The explanation is the following: the dynamic equations of a robot manipulator do not depend on the angle of the first joint [8]; in other words, the first joint is always cyclic. On the other hand, in the absence of gravity, the acceleration constraints imposed on a fixed-base manipulator by a cyclic joint are integrable to velocity constraints [6]. Consequently, the acceleration constraints imposed by the spherical joint of the DEM can be integrated to velocity constraints, which turn out to be identical to the SM's conservation of angular momentum. With this remark we hope to bridge the gap, up to now unexplored, between the research on underactuated manipulators and space manipulator systems. Hopefully, control techniques developed for one category will be useful for the other and vice-versa.

7 Effect of model uncertainty

Since the DEM parameters are computed for a given SM model, uncertainties in the later will naturally produce errors in the former. In this section, we study how the modeling error affects the mapping between the two systems., and the degree to which parameter uncertainty on each of the SM's links reflects as errors on each of the DEM's links.

From the definition of the DEM (18), we know what SM parameters affect what DEM parameters, and we can quantitatively compute the error mapping as either the ratio between the absolute or relative errors of the SM parameters and those of the DEM. Let y_i represent any geometric or dynamic parameter of the DEM's i-th link, and dy_i its corresponding uncertainty. Such parameter is a function of one more of the SM's parameters; for example, m_i' is a function of all m_i, or, of the vector $\mathbf{m}$. We will represent the error mapping by relations of the form

$$d\mathbf{y} = F \begin{bmatrix} d\mathbf{m} \\ d\mathbf{I} \\ d\mathbf{R} \\ d\mathbf{L} \end{bmatrix} \tag{72}$$

with the matrix F having appropriate subscripts to distinguish different cases. We will use $\hat{F}$ to represent the matrix mapping the relative errors from the SM parameters to the DEM ones.

We start with the simplest of the mappings from the SM parameters to the DEM ones, namely, the computation of the DEM's inertia tensors. From (18) one can see that $I_i^{'}$ depends only on the value of I_i, and that:

$$F_{dI} = I_{(n+1)\times(n+1)} \tag{73}$$

$$\hat{F}_{dI} = I_{(n+1)\times(n+1)} \tag{74}$$

where $F_{dI}(i,j) = \frac{\partial I_i^{'}}{\partial I_j}$, $\hat{F}_{dI}(i,j) = \frac{\partial I_i^{'}/I_i^{'}}{\partial I_j/I_j}$, and $I_{(n+1)\times(n+1)}$ represents the $(n+1)\times(n+1)$ identity matrix.

The error mapping for the DEM's links masses is more complex, for uncertainties on the value of $m_i^{'}$ are a consequence of uncertainties on the values of all m_i, $i = 1,\ldots,n+1$. When $j > i$,

$$\frac{\partial m_i^{'}}{\partial m_j} = 2\frac{M_t m_i}{\sum_{k=1}^{i-1} m_k \sum_{k=1}^{i} m_k}. \tag{75}$$

When $j = i$,

$$\begin{aligned} \frac{\partial m_i^{'}}{\partial m_j} &= \frac{\partial m_i^{'}}{\partial m_i} \\ &= 2\frac{M_t m_i}{\sum_{k=1}^{i-1} m_k \sum_{k=1}^{i} m_k} + \left(\frac{M_t}{\sum_{k=1}^{i} m_k}\right)^2. \end{aligned} \tag{76}$$

Finally, when $j < i$,

$$\frac{\partial m_i^{'}}{\partial m_j} = -\frac{M_t m_i}{\sum_{k=1}^{i-1} m_k \sum_{k=1}^{i} m_k}\left(\frac{M_t m_i}{\sum_{k=1}^{i-1} m_k \sum_{k=1}^{i} m_k} + \frac{2\sum_{k=i+1}^{n+1} m_k}{\sum_{k=1}^{i} m_k}\right). \tag{77}$$

The above equalities can be written in matrix form as:

$$d\mathbf{m}^{'} = F_{dm} d\mathbf{m} \tag{78}$$

where $F_{dm}(i,j) = \frac{\partial m_i^{'}}{\partial m_j}$. The matrix F_{dm} has following properties:

Property 1: The diagonal and upper triangular elements are positive; the lower triangular elements are negative, and

$$\begin{array}{lcll} F_{dm}(1,j) &=& 0, & j = 1,2,\ldots,n+1, \\ F_{dm}(i,j) &=& F_{dm}(i,i-1) < 0, & i < j, \\ F_{dm}(i,j) &=& F_{dm}(i,i+1) > 0, & i > j, \\ F_{dm}(i,i) &>& F_{dm}(i,i+1) > 0, & i = 1,2,\ldots,n+1. \end{array} \tag{79}$$

Property 2: If

$$\begin{cases} K = \dfrac{M_t}{\sum\limits_{k=1}^{i} m_k} < 2, \\ m_i < \left(\dfrac{4}{K} - 2\right) \sum\limits_{k=1}^{i-1} m_k, \end{cases} \tag{80}$$

then

$$\|F_{dm}(i, i-1)\| < \|F_{dm}(i, i+1)\|, \tag{81}$$

i.e., the DEM's i-th link mass value is affected more strongly by errors on the SM's $(i-1)$-th link than by errors on the SM's $(i+1)$-th link. Otherwise,

$$\|F_{dm}(i, i-1)\| > \|F_{dm}(i, i+1)\|. \tag{82}$$

Property 3: If

$$\begin{cases} \sum\limits_{k=1}^{i} m_k > \frac{3}{4} M_t, \\ m_1 \geq \frac{M_t}{2}, \end{cases} \tag{83}$$

then

$$\|F_{dm}(i, i-1)\| < \|F_{dm}(i, i+1)\|. \tag{84}$$

The above analysis can be repeated for the ratio of the relative errors if we compute the elements of $\hat{F}_{dm}$, where $\hat{F}_{dm}(i,j) = \left(\frac{\partial m_i'}{\partial m_j}\right) \frac{m_j}{m_i'}$ and

$$\begin{aligned} \hat{F}_{dm}(i,j) &= \tfrac{2m_j}{M_t}, && j > i, \\ \hat{F}_{dm}(i,j) &= \tfrac{2m_j}{M_t} + \dfrac{\sum\limits_{k=1}^{i-1} m_k}{\sum\limits_{k=1}^{i} m_k} = 1 + m_i \left(\tfrac{2}{M_t} - \dfrac{1}{\sum\limits_{k=1}^{i} m_k} \right), && j = i, \\ \hat{F}_{dm}(i,j) &= \tfrac{2m_j}{M_t} \left(\dfrac{M_t m_i}{\sum\limits_{k=1}^{i-1} m_k \sum\limits_{k=1}^{i} m_k} + \dfrac{2 \sum\limits_{k=i+1}^{n+1} m_k}{\sum\limits_{k=1}^{i} m_k} \right), && j < i, \end{aligned} \tag{85}$$

Note that if $\sum\limits_{k=1}^{i} m_k > \frac{M_t}{2}$, then $\hat{F}_{dm}(i,i) > 1$.

Uncertainties on the location of the center of mass of the DEM links as a function of the errors on the SM's masses and link geometry can be written as:

$$d\mathbf{l}_c = \begin{bmatrix} F_{dl_c m} & F_{dl_c L} \end{bmatrix} \begin{bmatrix} d\mathbf{m} \\ d\mathbf{L} \end{bmatrix}, \tag{86}$$

where $F_{dl_cm}(i,j) = \frac{\partial l_{ci}}{\partial m_j}$, and $F_{dl_cL}(i,j) = \frac{\partial l_{ci}}{\partial L_j}$. The elements of the error mapping matrix F are given by:

$$\begin{aligned} F_{dl_cm}(1,j) &= 0, & j = 1,2,\ldots,n+1, \\ F_{dl_cm}(i,j) &= \frac{\sum_{k=i}^{n+1} m_k}{M_t^2}\mathbf{L}_i, & j < i, \\ F_{dl_cm}(i,j) &= -\frac{\sum_{k=1}^{i-1} m_k}{M_t^2}\mathbf{L}_i, & j \geq i, \end{aligned} \tag{87}$$

and

$$\begin{aligned} F_{dl_cL}(i,j) &= 0, & j \neq i, \\ F_{dl_cL}(i,j) &= \frac{\sum_{k=1}^{i-1} m_k}{M_t}, & j = i. \end{aligned} \tag{88}$$

As for the relative errors we can compute $\hat{F}_{dl_c} = \left[\begin{array}{cc} \hat{F}_{dl_cm} & \hat{F}_{dl_cL} \end{array} \right]$ where $\hat{F}_{l_cm}(i,j) = \left(\frac{\partial l_{ci}}{\partial m_j}\right)\frac{m_j}{l_{ci}}$, $\hat{F}_{l_cL}(i,j) = \left(\frac{\partial l_{ci}}{\partial L_j}\right)\frac{L_j}{l_{ci}}$,

$$\begin{aligned} \hat{F}_{l_cm}(1,j) &= 0, & j = 1,2,\ldots,n+1, \\ \hat{F}_{l_cm}(i,j) &= \frac{m_j \sum_{k=j}^{n+1} m_k}{M_t \sum_{k=1}^{j-1} m_k}, & j < i, \\ \hat{F}_{l_cm}(i,j) &= -\frac{m_j}{M_t}, & j \geq i, \end{aligned} \tag{89}$$

and

$$\begin{aligned} \hat{F}_{l_cL}(i,j) &= 0, & j \neq i, \\ \hat{F}_{l_cL}(i,j) &= 1, & j = i. \end{aligned} \tag{90}$$

Finally, uncertainties on the value of the DEM links' length is due to errors on both the SM's mass and its geometry:

$$d\mathbf{W} = \left[\begin{array}{ccc} F_{dWm} & F_{dWL} & F_{dWR} \end{array} \right] \left[\begin{array}{c} d\mathbf{m} \\ d\mathbf{L} \\ d\mathbf{R} \end{array} \right], \tag{91}$$

where $F_{dWm}(i,j) = \frac{\partial W_i}{\partial m_j}$, $F_{dWL}(i,j) = \frac{\partial W_i}{\partial L_j}$, $F_{dWR}(i,j) = \frac{\partial W_i}{\partial R_j}$, and

$$
\begin{aligned}
F_{dWm}(1,1) &= \frac{\sum_{k=2}^{n+1} m_k}{M_t^2}\mathbf{R}_1, \\
F_{dWm}(1,j) &= -\frac{\sum_{k=1}^{i} m_k}{M_t^2}\mathbf{R}_1, && j>1, \\
F_{dWm}(i,i) &= -\frac{\sum_{k=1}^{i-1} m_k}{M_t^2}\mathbf{L}_i + \frac{\sum_{k=i+1}^{n+1} m_k}{M_t^2}\mathbf{R}_i, \\
F_{dWm}(i,j) &= \frac{\sum_{k=i}^{n+1} m_k}{M_t^2}\mathbf{L}_i + \frac{\sum_{k=i+1}^{n+1} m_k}{M_t^2}\mathbf{R}_i, && j<i, \\
F_{dWm}(i,j) &= -\frac{\sum_{k=1}^{i-1} m_k}{M_t^2}\mathbf{L}_i - \frac{\sum_{k=1}^{i} m_k}{M_t^2}\mathbf{R}_i, && j>i,
\end{aligned}
\tag{92}
$$

$$
\begin{aligned}
F_{dWR}(i,j) &= 0, && j \neq i, \\
F_{dWR}(i,j) &= \frac{\sum_{k=1}^{i} m_k}{M_t}, && j=i,
\end{aligned}
\tag{93}
$$

$$
F_{dWL} = F_{dlcL}. \tag{94}
$$

The above analysis can be repeated for the ratio of the relative errors by computing the elements of $\hat{F}_{Wm}$, $\hat{F}_{WL}$, $\hat{F}_{WR}$, where $\hat{F}_{Wm}(i,j) = \left(\frac{\partial W_i}{\partial m_j}\right)\frac{m_j}{W_i}$, $\hat{F}_{WL}(i,j) = \left(\frac{\partial W_i}{\partial L_j}\right)\frac{L_j}{W_i}$, $\hat{F}_{Wm}(i,j) = \left(\frac{\partial W_i}{\partial R_j}\right)\frac{R_j}{W_i}$.

8 Case study

To illustrate the equivalence between the SM and its corresponding DEM, we selected a planar SM equipped with a 2-link rotary manipulator . The corresponding DEM is a fixed-base 3-link planar rotary manipulator whose first joint is passive. The equivalence between the SM and the DEM will be shown in two different ways. First, we will apply the same open-loop torque to the SM's manipulator and to joints 2 and 3 of the DEM. With this experiment we intend to demonstrate that the kinematic behavior (e.g. the location of the end-effector in inertial space) and the dynamic behavior (e.g. the joint angles and base rotation) of both systems are identical. Second, we will perform a closed-loop control experiment in joint space, driving both SM's actuators and the DEM's joints 2 and 3 to a specified set-point. With this experiment we intend to demonstrate that, when under the action of the same controller with the same control gains, the SM and DEM behave identically.

8.1 Dynamic modeling

Table 1 presents the kinematic and dynamic parameters selected for the SM. Table 2 presents the corresponding parameters of the DEM.

Table 1: Geometric and dynamic parameters of the 2-link SM.

LINK	$L_i(m)$	$R_i(m)$	$m_i(kg)$	$I_i(kg \cdot m^2)$
1	-	0.5	4	0.4
2	0.5	0.5	1	0.1
3	0.5	0.5	1	0.1

Table 2: Geometric and dynamic parameters of the 3-link DEM.

LINK	$W_i(m)$	$lc_i(m)$	$m_i(kg)$	$I_i(kg \cdot m^2)$
1	0.333	0.0	4	0.4
2	0.750	0.333	1.8	0.1
3	0.917	0.417	1.2	0.1

The SM dynamic equations are expressed as:

$$M\ddot{\mathbf{q}} + h(\mathbf{q}, \dot{\mathbf{q}}) = \begin{bmatrix} 0 \\ \tau_2 \\ \tau_3 \end{bmatrix}, \tag{95}$$

where M and h are detailed in Appendix A.

The DEM dynamic equations are given by:

$$M'\ddot{\mathbf{q}}' + h'(\mathbf{q}', \dot{\mathbf{q}}') = \begin{bmatrix} 0 \\ \tau_2' \\ \tau_3' \end{bmatrix}, \tag{96}$$

where M' and h' detailed in Appendix B.

8.2 Open-loop control experiment

We applied sinusoidal torques with amplitude 0.5 Nm and period 1 s to both SM's actuators and the DEM's joints 2 and 3 (see Figure 5). Figures 6 and 7 present the results, showing that (i) the joint angles trajectories of both systems (including the rotation of the base) are identical; (ii) the trajectories of both end-effectors in inertial space are identical. We measured the maximum error between these quantities, and verified that: (i) the maximum deviation between q_i and q_i', $i = 1, 2, 3$ was equal to 1.7 seconds of arc (or 4.75×10^{-4} degrees);

(ii) the maximum deviation between the inertial location of the SM and DEM end-effectors was 0.016 mm. These errors are due to the fact that the dimensions of links 1 and 3 of the DEM are recurring decimals, which are represented in truncated form inside the computer program. This experiment confirms the kinematic and dynamic equivalence between the SM and the DEM.

8.3 Closed-loop control experiment

In this experiment we control the angles of both joints of the SM's manipulator to a constant set-point. Let $\theta_{23} = \begin{bmatrix} q_2 & q_3 \end{bmatrix}^T$; factoring out $\ddot{q}_1$ in the first line of (95) and substituting the result in the second and third lines, we obtain the open-loop relationship between the driving torques and the controlled joint angles:

$$\begin{aligned} \begin{bmatrix} \tau_2 \\ \tau_3 \end{bmatrix} &= \begin{bmatrix} M(2,2) - k_1 M(1,2) & M(2,3) - k_1 M(1,3) \\ M(3,2) - k_2 M(1,2) & M(3,3) - k_2 M(1,3) \end{bmatrix} \ddot{\theta}_{23} + \begin{bmatrix} h(2) - k_1 h(1) \\ h(3) - k_2 h(1) \end{bmatrix} \\ &= M_\tau \ddot{\theta}_{23} + h_\tau, \end{aligned} \tag{97}$$

where $k_1 = M(1,1)/M(2,1), k_2 = M(1,1)/M(3,1)$.

We selected a variable structure controller (VSC) to control the SM's actuators. To this end we define the 2-dimensional sliding surface

$$s = \Gamma \tilde{\theta}_{23} + \dot{\tilde{\theta}}_{23}, \tag{98}$$

where Γ is a diagonal matrix with positive entries, and $\tilde{z}$ represents the error on the variable z between its current value and its desired value z^d. The following is the reference acceleration of the actuators that guarantee that the state space trajectories converge to the sliding surface $s = 0$ and then to the origin of the state space:

$$\ddot{\theta}^r = \Gamma \dot{\tilde{\theta}}_{23} + \ddot{\theta}^d_{23} + P sgn(s), \tag{99}$$

where P is a diagonal matrix with positive entries. The control torque is obtained by substituting (99) in (97). To eliminate the chattering introduced by the term $sgn(s)$ in (99) we add a boundary layer around the sliding surface $s = 0$, i.e., we substitute $sgn(s)$ by the saturation function $sat(s)$ defined by:

$$sat(x) = \begin{cases} sgn(x), & \text{if } x \geq \varepsilon; \\ \frac{x}{\varepsilon}, & \text{if } x < \varepsilon. \end{cases} \tag{100}$$

The control gains were selected as $P = diag(10, 10)$, $\Gamma = diag(5, 5)$, $\epsilon = diag(0.3, 0.3)$. The torques computed for the control of the SM were applied to both the SM and the DEM

(see Figure 8). The desired joint angles were chosen as $\theta_{23}^d = [\ 30^o \quad -30^o\ ]^T$. Figure 9 shows the resulting joint trajectories, including the rotation of the base. As we can see, the SM and the DEM behave identically when under the action of the same controller. The maximum deviation between the joint angles is equal to 0.29 seconds of arc (8.1×10^{-5} degrees) and the maximum deviation between the end-effector locations is 0.0028 mm. This experiment demonstrates that it is possible to simulate the behavior of a complex free-floating space manipulator system through the control of a simple, easy-to-assemble fixed-base manipulator with a passive joint at the base.

8.4 Error mapping

We close this case study analyzing the influence of modeling errors on the SM parameters on the mass, length, and location of the center of mass of the DEM's second link (naturally, the analysis can be repeated for the other 2 links). We adopted absolute errors with magnitude varying from 0 to 0.1 (Kg or m), and relative errors with magnitude varying from 0 to 10

Figure 10 shows the absolute error on $m_2^{'}$ given absolute errors on $m_i, i = 1, 2, 3$. As expected, from the slopes of the error mapping surfaces one can see that $dm_2^{'}$ is much more influenced by errors in m_2 than by errors in m_3 (recall that $F_{dm}(2,2) > F_{dm}(2,3)$ according to Property 1). Additionally, one can see that $dm_2^{'}$ is inversely proportional to dm_1, a property that agrees with the fact that $F_{dm}(2,1) < 0$. Identical conclusions can be drawn from Figure 11, where we show the relative error $dm_2^{'}/m_2^{'}$ for given relative errors $dm_i/m_i, i = 1, 2, 3$.

Figure 12 shows the absolute error on the location of the center of mass of link 2, l_{c2}, for given absolute errors in the SM masses and L_2 (recall that $F_{dlcL}(i,j) = 0 for i \neq j$). That figure consists of 9 surfaces divided into groups, the lowermost corresponding to $dL_2 = 0.1$ m, the middle one to $dL_2 = 0$ m, and the uppermost to $dL_2 = -0.10$ m. Within each group dm_1 varies (from top to bottom) from 0.1 Kg to -0.1 Kg. One can see that the influence of the $dm_i, i = 1, 2, 3$ on dl_{c2} is very small when compared to the influence of dL_2. The same fact can be seen on Figure 13, where we show the absolute error on dW_2 given absolute errors on the SM masses and geometry. We can conclude that, for this particular space manipulator system, errors on the masses of each of the DEM links are mostly due to errors on the masses of the corresponding SM link; and that errors on the DEM kinematic parameters (l_{ci} and W_i) are mostly due to errors on the SM kinematic parameters (R_i and L_i).

The foregoing analysis will be of utmost importance when one designs a fixed-base manipulator to represent a given SM. If the designer knows the uncertainty bounds on the DEM parameters, (s)he can find out the corresponding errors on the SM parameters using a set

of curves like the ones shown in Figures 10-13. With these, (s)he can decide whether or not the SM modeling errors are acceptable and either redesign the DEM or make use of robust controllers to cope with the uncertainties.

Finally, the error mapping analysis can also be used to guide the design of the DEM. For example, from Appendix B, one can see that l_{c1} appears only in $M'(1,1)$ and not in the other elements of M'; and it is multiplied by the mass of the DEM's first link. If the value l_{c1} has a substantial uncertainty, the equivalence between the SM and the DEM may still be kept if one designs the DEM's first link as light as possible. (Note that its inertia should be equal to that of the SM's first link, the base).

9 Conclusion

We propose in this paper the novel concept of the DEM, the Dynamically Equivalent Manipulator. The DEM has several advantages: (1) it is real in nature and can be built from off-the-shelf components for realistic experiments in the laboratory. The concept is different from the VM, which is an idealized massless kinematic chain; (2) The DEM can be used as a tool for dynamic modeling of space manipulators, based on Lagrangian dynamics or any other formulation used for fixed-base, conventional manipulators; (3) control methods developed for fixed-base manipulators can be easily examined for feasibility of use in space manipulator systems through the DEM; (4) the DEM concept can be extended to represent attitude-controlled SM's; in this case the corresponding DEM is a fixed-base manipulator whose first joint is an actively controlled spherical one; (5) The DEM concept bridges the gap between space manipulator systems and fixed-base underactuated manipulators; it allows control methods developed for the former to be applied to the later and vice-versa.

10 Acknowledgments

The third author is partially sponsored by the Brazilian National Council for Research and Development (CNPq).

Appendix A: Dynamic model of a 2-link space manipulator

The elements of the inertia matrix of the free-floating SM equipped with a 2-link manipulator are given by:

$$\begin{aligned} M(3,3) &= S_{cc} + I_3, \\ M(2,3) &= M(3,2) = M(3,3) + S_{bc}c_3, \\ M(1,3) &= M(3,1) = M(2,3) + S_{ac}c_{23}, \\ M(2,2) &= M(2,3) + S_{bb} + I_2 + S_{bc}s_3, \\ M(1,2) &= M(2,1) = M(2,2) + S_{ab}c_2 + S_{ac}c_{23}, \\ M(1,1) &= M(1,2) + S_{aa} + I_1 + S_{ab}c_2 + S_{ac}c_{23}. \end{aligned} \tag{A1}$$

where

$$\begin{aligned} S_{aa} &= \tfrac{1}{M_t} m_1(m_2+m_3)R_1^2, \\ S_{bb} &= \tfrac{1}{M_t}[m_1(m_2+m_3)L_2^2 + (m_1+m_2)m_3R_2^2 + 2m_1m_3L_2R_2], \\ S_{cc} &= \tfrac{1}{M_t}(m_1+m_2)m_3L_3^2, \\ S_{ab} &= \tfrac{1}{M_t} m_1[(m_2+m_3)L_2 + m_3R_2]R_1, \\ S_{ac} &= \tfrac{1}{M_t} m_1m_3R_1L_3, \\ S_{bc} &= \tfrac{1}{M_t}[m_1L_2 + (m_1+m_2)R_2]m_3L_3. \end{aligned} \tag{A2}$$

The non-inertial torques are given by:

$$h(i) = \sum_{j=1}^{3}\sum_{k=1}^{3} h_{ijk}\dot{q}_j\dot{q}_k, \qquad i = 1,2,3. \tag{A3}$$

where

$$\begin{aligned} h_{111} &= 0, \\ h_{122} &= -S_{ab}s_2 - S_{ac}s_{23}), \\ h_{133} &= -S_{bc}s_3 + S_{ac}s_{23}), \\ h_{112} &+ h_{121} = 2h_{122}, \\ h_{113} &+ h_{131} = 2h_{133}, \\ h_{123} &+ h_{132} = 2h_{133}, \\ h_{211} &= -h_{122}, \\ h_{222} &= 0, \\ h_{233} &= -S_{bc}s_3, \\ h_{212} &+ h_{221} = 0, \\ h_{213} &+ h_{231} = 2h_{233}, \\ h_{223} &+ h_{232} = 2h_{233}, \\ h_{311} &= -h_{133}, \\ h_{322} &= -h_{233}, \\ h_{333} &= 0, \\ h_{312} &+ h_{321} = 2h_{322}, \\ h_{313} &+ h_{331} = 0, \\ h_{323} &+ h_{332} = 0. \end{aligned} \tag{A4}$$

Appendix B: Dynamic model of a 3-link DEM

The elements of the inertia matrix of the 3-link DEM are given by:

$$\begin{aligned}
M'(1,1) &= m_1' l_{c1}^2 + I_1' + m_2'(W_1^2 + l_{c2}^2 + 2W_1 l_{c2} c_2') + I_2' \\
&\quad + m_3'(W_1^2 + W_2^2 + l_{c3}^2 + 2W_1 W_2 c_2' + 2W_2 l_{c3} c_3' + 2W_1 l_{c3} c_{23}') + I_3', \\
M'(2,2) &= m_2' l_{c2}^2 + I_2' + m_3'(W_2^2 + l_{c3}^2 + 2W_2 l_{c3} c_3') + I_3', \\
M'(3,3) &= m_3' l_{c3}^2 + I_3', \\
M'(1,2) &= M'(2,1) \\
&= m_2'(l_{c2}^2 + W_1 l_{c2} c_2') + I_2' + m_3'(W_2^2 + l_{c3}^2 + W_1 W_2 c_2' \\
&\quad + 2W_2 l_{c3} c_3' + W_1 l_{c3} c_{23}') + I_3', \\
M'(1,3) &= M'(3,1) m_3'(l_{c3}^2 + W_2 l_{c3} c_3' + W_1 l_{c3} c_{23}') + I_3', \\
M'(2,3) &= M'(3,2) m_3'(l_{c3}^2 + W_2 l_{c3} c_3') + I_3'.
\end{aligned} \tag{B1}$$

The non-inertial torques are given by:

$$h'(i) = \sum_{j=1}^{3} \sum_{k=1}^{3} h_{ijk}' \dot{q}_j' \dot{q}_k', \qquad i = 1, 2, 3. \tag{B2}$$

where

$$\begin{aligned}
h_{111}' &= 0, \\
h_{122}' &= -m_2' W_1 l_{c2} s_2' - m_3'(W_1 W_2 s_2' + W_1 l_{c3} s_{23}'), \\
h_{133}' &= -m_3'(W_2 l_{c3} s_3' + W_1 l_{c3} s_{23}'), \\
h_{112}' &+ h_{121}' = 2h_{122}', \\
h_{113}' &+ h_{131}' = 2h_{133}', \\
h_{123}' &+ h_{132}' = 2h_{133}', \\
h_{211}' &= -h_{122}', \\
h_{222}' &= 0, \\
h_{233}' &= -m_3' W_2 l_{c3} s_3', \\
h_{212}' &+ h_{221}' = 0, \\
h_{213}' &+ h_{231}' = 2h_{233}', \\
h_{223}' &+ h_{232}' = 2h_{233}', \\
h_{311}' &= -h_{133}', \\
h_{322}' &= -h_{233}', \\
h_{333}' &= 0, \\
h_{312}' &+ h_{321}' = 2h_{322}', \\
h_{313}' &+ h_{331}' = 0, \\
h_{323}' &+ h_{332}' = 0.
\end{aligned} \tag{B3}$$

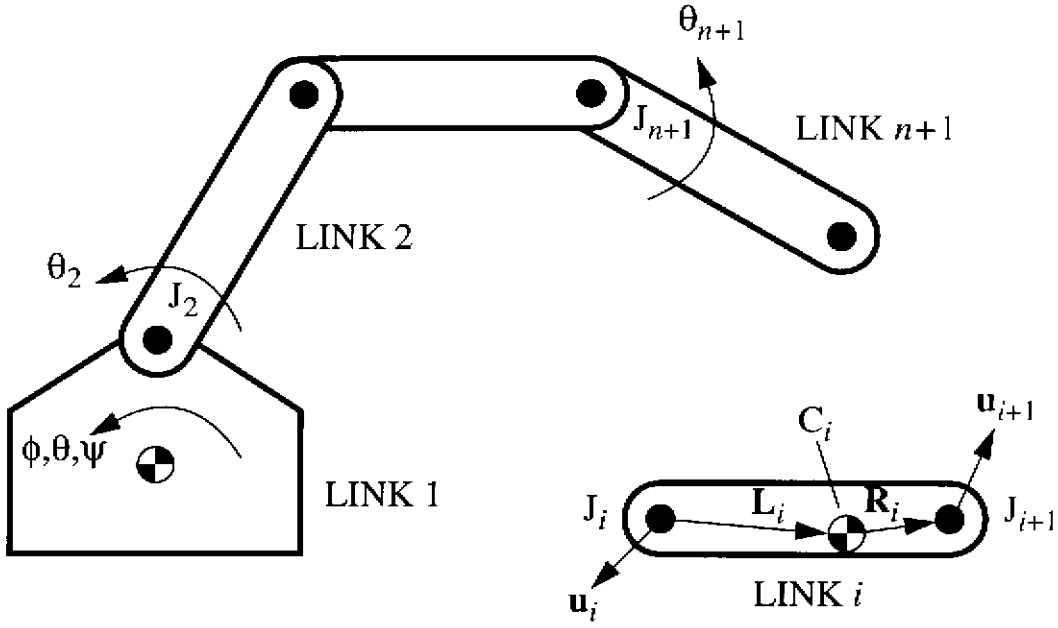

Figure 1: The space manipulator system (SM), composed of a robot manipulator mounted on a free-floating base.

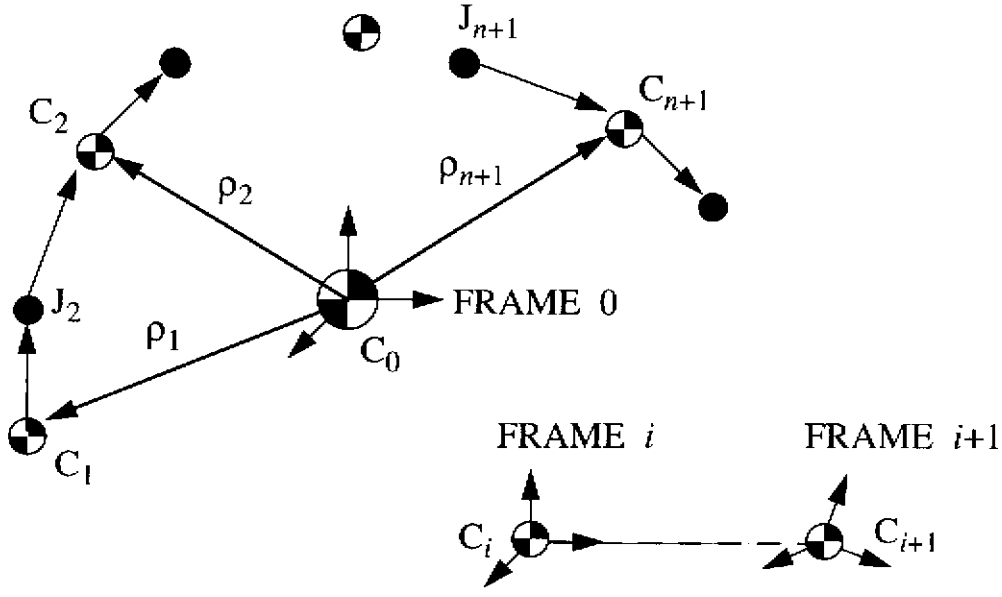

Figure 2: Coordinate frames attached to the the SM's links.

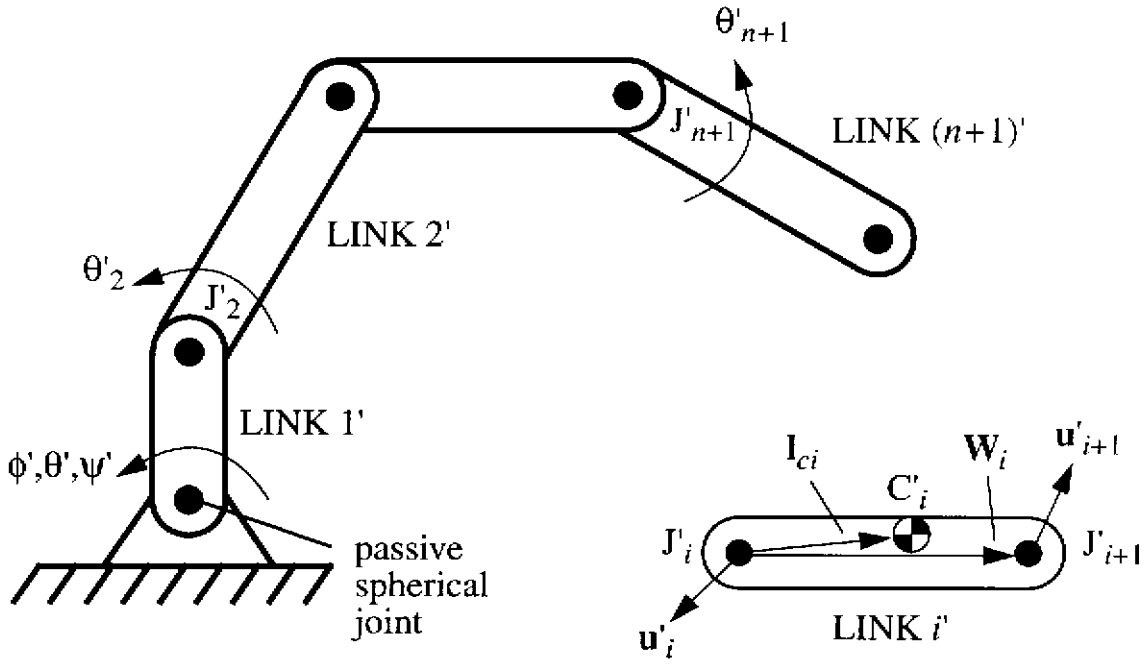

Figure 3: Fixed-base robot manipulator with a passive spherical joint at the base.

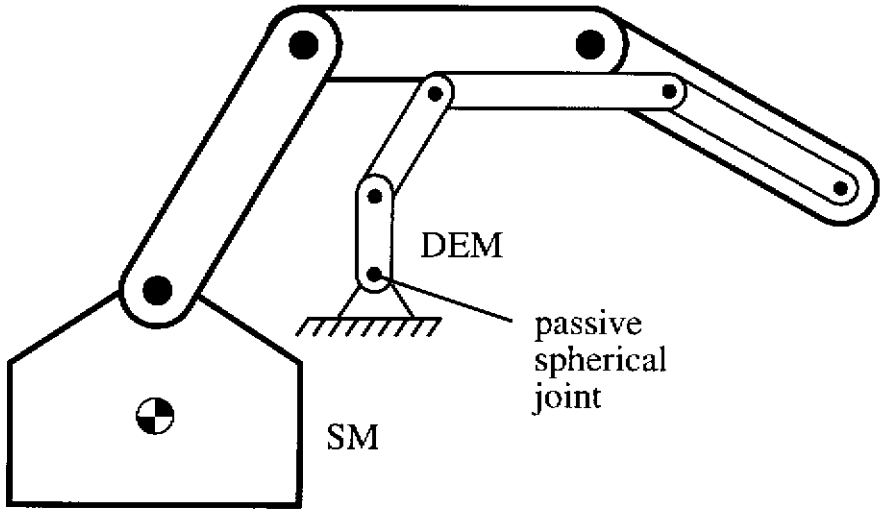

Figure 4: The SM and its corresponding DEM.

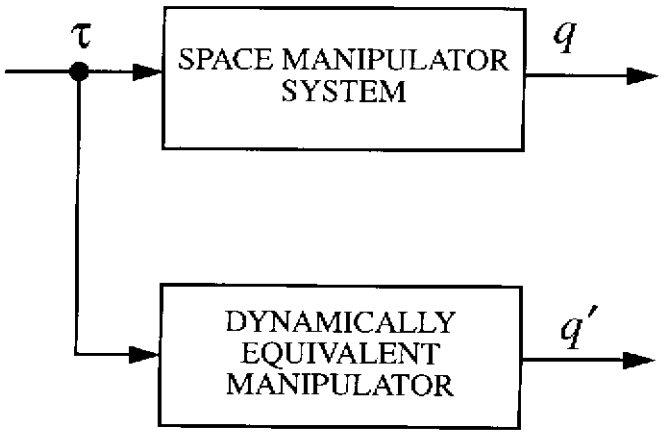

Figure 5: Open-loop control experiment block diagram.

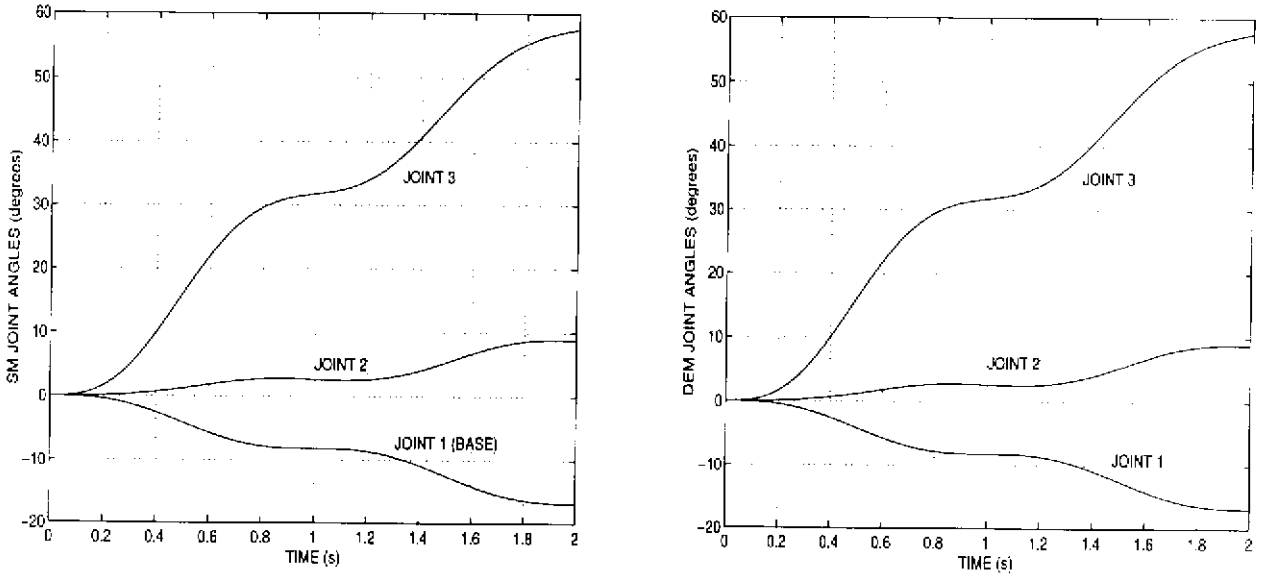

Figure 6: SM and DEM joint angles when a sinusoidal open-loop torque is applied to their actuators.

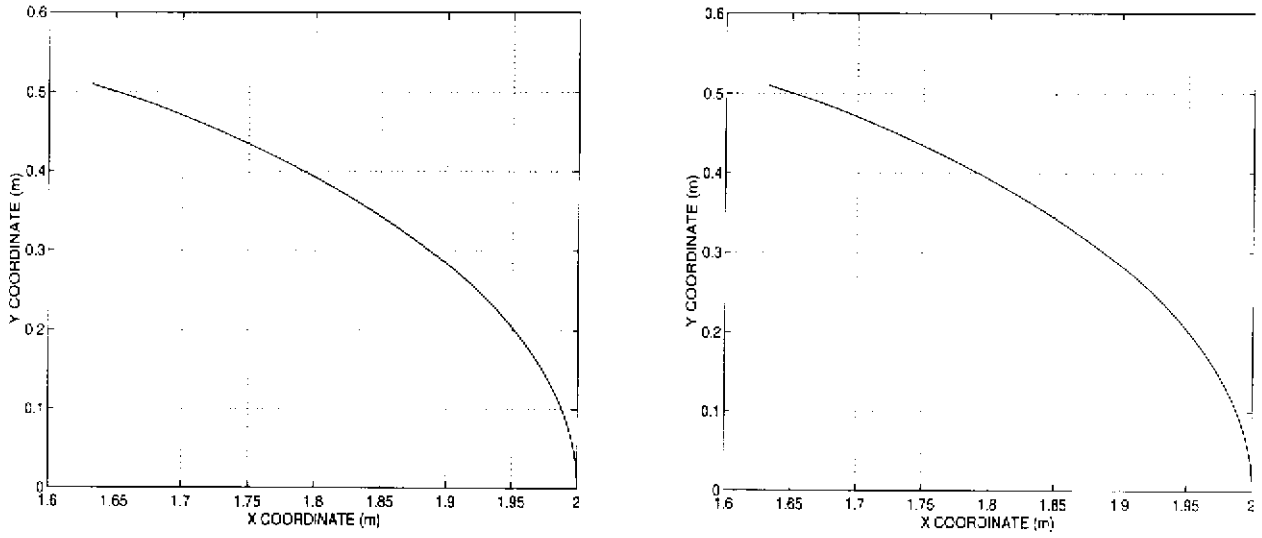

Figure 7: SM and DEM end-effector positions when a sinusoidal open-loop torque is applied to their actuators.

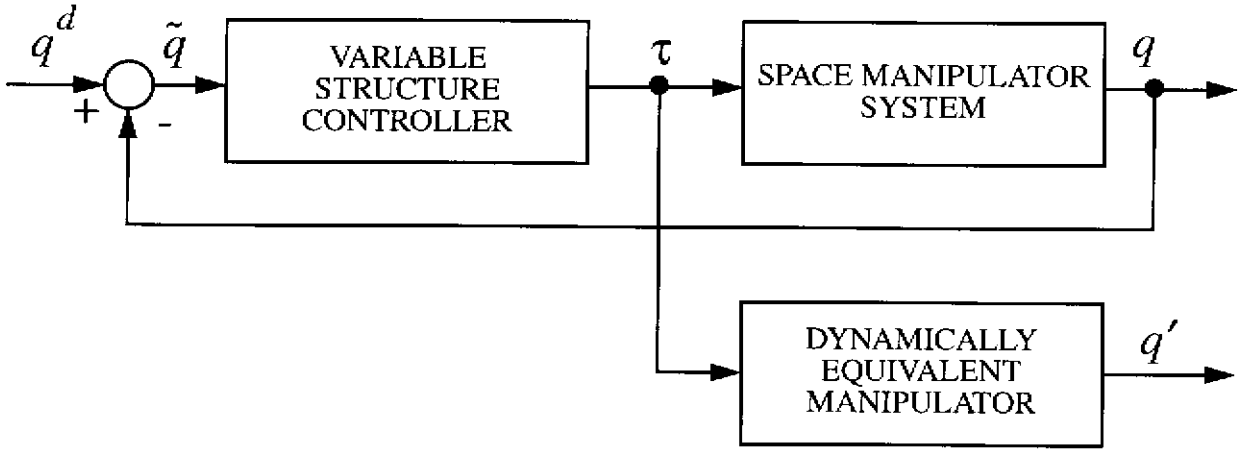

Figure 8: Closed-loop control experiment block diagram.

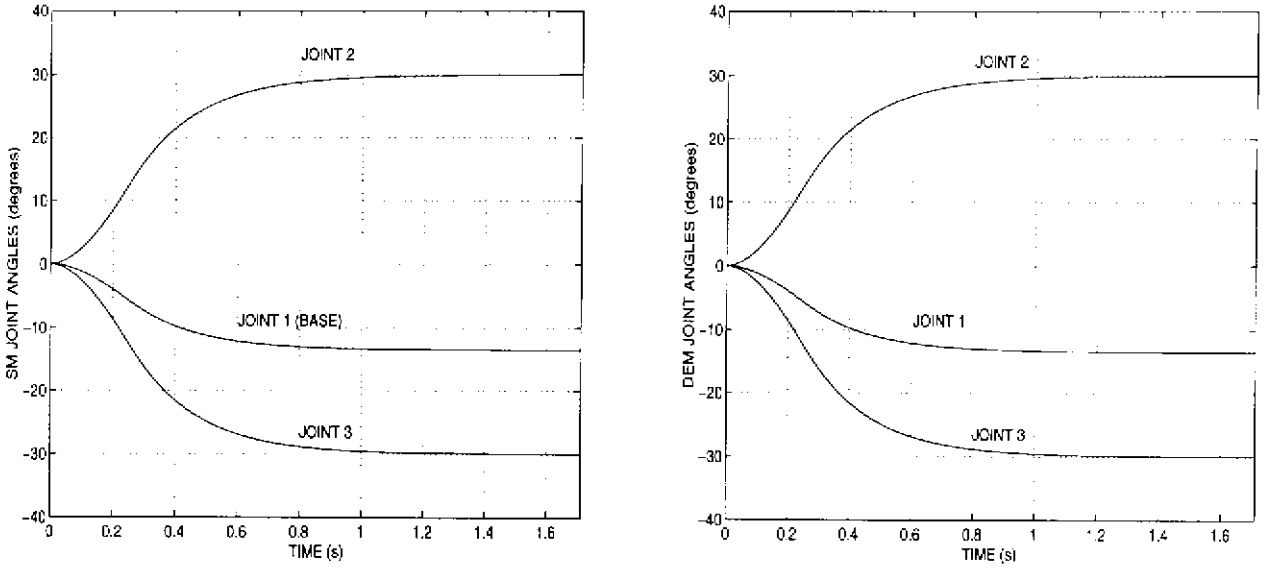

Figure 9: SM and DEM closed-loop joint angles.

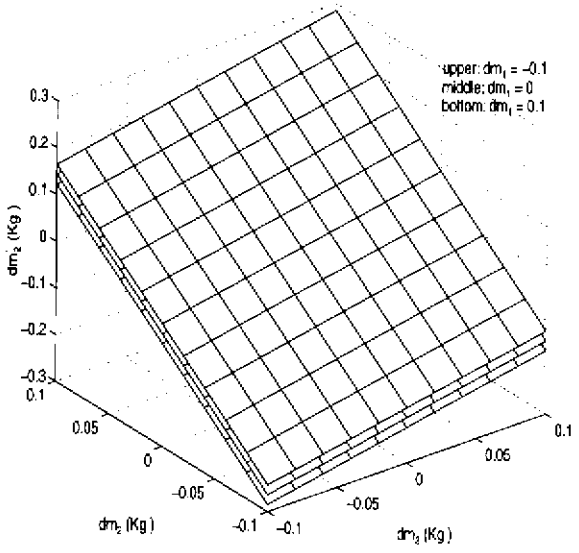

Figure 10: Absolute error mapping (in Kg) from the masses of the SM links to the mass of the DEM second link.

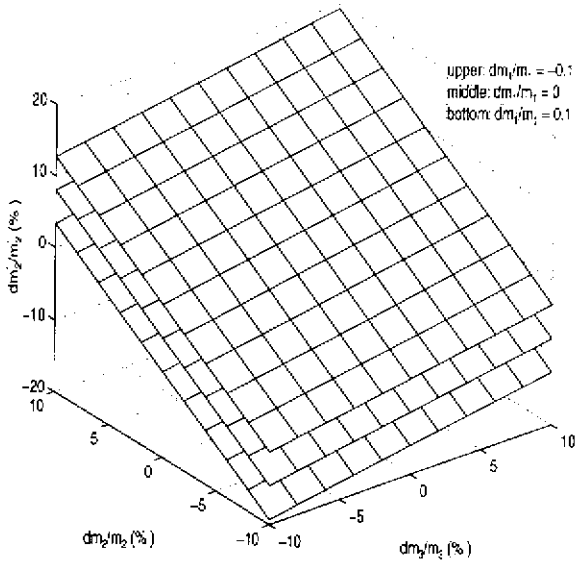

Figure 11: Relative error mapping (in %) from the masses of the SM links to the mass of the DEM second link.

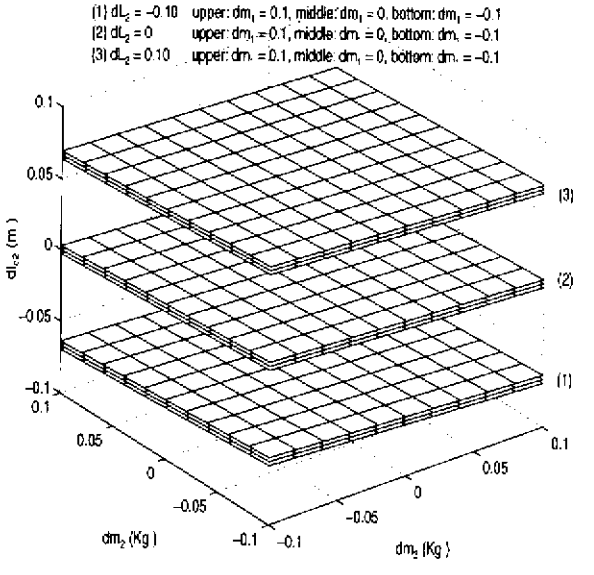

Figure 12: Absolute error mapping (in m) from the masses and geometry of the SM links to the location of the center of mass of the DEM second link.

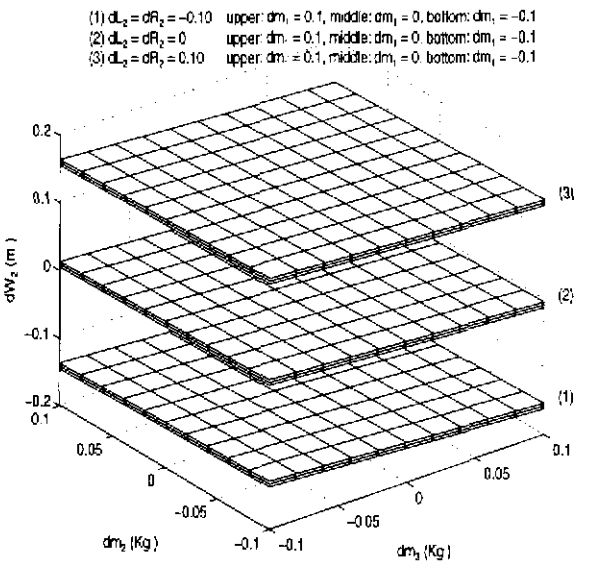

Figure 13: Absolute error mapping (in m) from the masses and geometry of the SM links to the length of the DEM second link.